Carbohydrate Polymers 87 (2012) 471–479

Contents lists available at ScienceDirect

Carbohydrate Polymers

journal homepage: www.elsevier.com/locate/carbpol

Diversity in the supramolecular interactions of 5,6-dichloro-2-(trifluoromethyl)-1*H*-benzimidazole with modified cyclodextrins: Implications for physicochemical properties and antiparasitic activity

Yareli Rojas-Aguirre[a], Ivan Castillo[b], David J. Hernández[b], Benjamín Nogueda-Torres[c], Adrián Márquez-Navarro[c], Juan C. Villalobos[c], Francisco Sánchez-Bartéz[a], Luvia Sánchez-Torres[c], Isabel Gracia-Mora[d], Rafael Castillo[a], Francisco Hernández-Luis[a,*]

[a] *Facultad de Química, Departamento de Farmacia, Universidad Nacional Autónoma de México, México, DF 04360, Mexico*
[b] *Instituto de Química, Universidad Nacional Autónoma de México, Circuito Exterior, Ciudad Universitaria, México, DF 04360, Mexico*
[c] *Escuela Nacional de Ciencias Biológicas, Instituto Politécnico Nacional, México, DF 11340, Mexico*
[d] *Facultad de Química, Departamento de Química Inorgánica y Nuclear, Universidad Nacional Autónoma de México, DF 04360, Mexico*

ARTICLE INFO

Article history:
Received 26 May 2011
Received in revised form 29 July 2011
Accepted 4 August 2011
Available online 11 August 2011

Keywords:
Benzimidazole
Cyclodextrins
Supramolecular association
Leishmania mexicana
Trypanosoma cruzi

ABSTRACT

The molecular interactions of 5,6-dichloro-2-(trifluoromethyl)-1*H*-benzimidazole (G2), an antiprotozoa with poor aqueous solubility, with 2-hydroxypropyl-α-cyclodextrin (HPαCD), methyl-β-cyclodextrin (MβCD) and 2-hydroxypropyl-β-cyclodextrin (HPβCD) were examined. The aqueous solubility enhancement by cyclodextrins (CDs) was evidenced in phase-solubility diagrams, and the stoichiometry of G2/CD systems was determined by Job's plots. Two-dimensional NMR spectroscopic data revealed that a different mode of interaction took place between G2 and CDs in solution. With HPαCD, a non-inclusion complex was generated. In the case of MβCD, a typical host–guest system was obtained and with HPβCD a partial inclusion complex through the narrow side of the macrocycle was formed. ESI-mass spectrometric data confirmed the stoichiometry and mode of interaction of these systems in solution. Solid-state characterization (scanning calorimetry and powder X-ray diffraction) supported the inclusion complex formation. The leishmanicidal activity, trypanocidal activity and non-toxic profile of G2/MβCD showed the advantages of using this inclusion complex to promote the biological assays extension of G2.

1. Introduction

Neglected tropical diseases (NTDs) are still a major public health concern for most developing countries (Renslo & McKerrow, 2006). Among these diseases, those caused by protozoa have great importance because some have reemerged over the last few decades as important threats to human health and economic development. According to their prevalence, there are 17 diseases currently listed as NTDs. Of great concern are leishmaniasis, caused by various *Leishmania* species, and American trypanosomiasis (also known as Chagas' disease and caused by *Trypanosoma cruzi*) which rank 5th and 6th in the list, respectively (Gyapong et al., 2010; Anonymous, 2011, http://www.who.int/neglected_diseases/diseases/en/). Both infections are widespread mostly in tropical and subtropical countries, with a worldwide incidence of more than 20 million affected people (Clayton, 2010; Coura & Pinto, 2009; Desjeux, 2004; Lannes-Vieira, Correia, Corrêa-Oliveira, & de Araújo-Jorge, 2009; Santos et al., 2008). In the absence of effective vaccines, chemotherapy plays a critical role in the control of these diseases. Pentavalent antimonials (e.g. Pentostam and Glucantime), Amphotericine B, and more recently Miltefosine, are used for leishmaniasis (Croft & Coombs, 2003; Natera et al., 2007; Santos et al., 2008). On the other hand, Benznidazole and Nifurtimox are drugs used to treat Chagas' disease (Croft, Barrett, & Urbina, 2005; Iatropoulos, Wang, von Keutz, & Williams, 2006; Maya et al., 2003). Besides limitations in terms of costs and difficulty of administration, the efficacy of these chemotherapeutic agents are variable, the treatment often causes severe side effects, and there is an increasing emergence of resistant strains. All these facts underline the urgent need for the development of new, safe, and easy-to-administer molecules for the treatment of these infectious diseases.

Following our ongoing project to develop new antiparasitic agents using the 2-(trifluoromethyl)-1*H*-benzimidazole system as a scaffold (Navarrete-Vázquez et al., 2001, 2003, 2006), we recently reported the synthesis of 5,6-dichloro-2-(trifluoromethyl)-1*H*-benzimidazole, in this work named G2 (Fig. 1), which presented

* Corresponding author. Tel.: +52 55 56225287; fax: +52 55 56225329.
E-mail addresses: franher@unam.mx, franher122@gmail.com (F. Hernández-Luis).

0144-8617/$ – see front matter © 2011 Elsevier Ltd. All rights reserved.
doi:10.1016/j.carbpol.2011.08.009

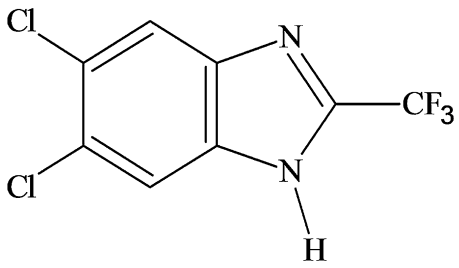

Fig. 1. Chemical structure of G2.

an interesting antiprotozoal profile due to its biological activity against *Giardia intestinalis*, *Entamoeba histolytica*, *Trichomonas vaginalis* and *Leishmania mexicana* (Hernández-Luis et al., 2010). However, G2 showed poor aqueous solubility, which hampered the biological assays and restricted the continuity of subsequent evaluations.

An alternative to increase the water solubility, stability, and bioavailability of drugs has been the formation of inclusion complexes with cyclodextrins (CDs) (Brewster & Loftsson, 2007; Carrier, Miller, & Ahmed, 2007; Loftsson & Duchêne, 2007; Loftsson, Hreinsdóttir, & Másson, 2005; Rojas-Aguirre et al., 2011). CDs are cyclic oligosaccharides formed by glucopyranose units bound through 1–4 bonds, and are most commonly composed by 6 (α-CD), 7 (β-CD) or 8 (δ-CD) glucose units. Due to the lack of free rotation about the bonds connecting the glucopyranose units, CDs are not perfectly cylindrical molecules but are cone shaped creating a hydrophobic micro-environment in the interior of the cavity, while the outer surface of the cone remains hydrophilic. Therefore, CDs act as hosts in the formation of inclusion complexes with appropriately sized molecules (guests); the resulting complexes generally offer a variety of physicochemical advantages over the free guest (Dodziuk, 2006; Tong & Wen, 2008). Furthermore, chemically modified CDs represent an excellent alternative for complexation of molecules since the dimensions of their cavities can be tailored, and their water solubility can be improved relative to parent CDs. Among modified CDs, HPβCD and MβCD appear to be especially useful based on their low toxicity, complexation potential, and water solubility (Brewster & Loftsson, 2007; Csempesz, Süle, & Puskás, 2010; Danel et al., 2008).

Considering the advantages provided by modified CDs, we prepared the G2/HPαCD, G2/MβCD and G2/HPβCD systems in order to enhance the aqueous solubility of G2 to extend its biological evaluation. The studies of molecular associations were obtained by phase-solubility diagrams and Job's plots. The association mode in solution was determined by one and two-dimensional ^{1}H NMR spectroscopy and ESI-mass spectrometry. Additionally, differential scanning calorimetry (DSC) and powder X-ray diffraction (XRD) were employed to characterize the complex in the solid state. Finally, the in vitro activity against *L. mexicana* and *T. cruzi* of free G2, G2/HPαCD, G2/MβCD and G2/HPβCD systems was evaluated and their cytotoxicity profiles were determined.

2. Materials and methods

2.1. Materials

We prepared the benzimidazole derivative G2 according to the method described earlier (Hernández-Luis et al., 2010). HPαCD and HPβCD, with an average MW of 1180 and 1380, respectively (both with a degree of molar substitution of 0.6) and MβCD with an average MW of 1310 (extent of labeling of 1.6–2.0 mol CH_3 per unit anhydroglucose) were purchased from Sigma–Aldrich. Other reagents and chemicals were of analytical reagent grade. All experiments were carried out using ultrapure water (MILLI Q-Millipore).

2.2. Complex preparation

The complexes were prepared according to the coevaporation method. An ethanolic solution of G2 was added to an aqueous solution of HPαCD, MβCD or HPβCD at 1:1 host/guest mole ratio (concentration 1 mM). The mixture was magnetically stirred at room temperature for 7 days. After this period, the solvent was evaporated to dryness at 45 °C under vacuum (Vacuubrand CVC2^{II}). The resulting solid was collected, pulverized and sieved (200 μm sieve). Physical mixtures (PM) were prepared in the same molar ratio (1:1) in a mortar for 5 min. The mixtures were then passed through a 200 μm sieve.

2.3. Determination of intrinsic solubility

The solubility profile of G2 and its complexes was determined by the shake-flask method (Baka, Comer, & Takács-Novák, 2008). Briefly, an aliquot of 5 mL of phosphate buffer solution, pH 7.4, was added to a glass vial containing 5 mg of G2 or its mass equivalent as a complex in order to have excess of solid. The vials were stirred during 48 h at 25 °C followed by a sedimentation period of 18 h for phase separation. The amount of dissolved compound was measured by UV spectrophotometry at 290 nm (Genesys10uv, Thermo). Three independent experiments were carried out.

2.4. Phase solubility diagram

To investigate the effect of CDs on the solubility of G2, phase solubility studies were performed according to the method established by Higuchi and Connors (1965). Briefly, aqueous solutions containing increasing concentrations of the three CDs were prepared (0.0002, 0.0004, 0.0006, 0.0008 and 0.001 M). A constant amount of G2 in five-fold molar excess relative to the highest concentration of CD solution was added to each CD solution and the resulting suspensions were stirred for 48 h at room temperature. After this period, the suspensions were filtered through 0.2 μm membranes (Millex, Millipore) and G2 concentration was analyzed using an UV spectrophotometer at 290 nm (Genesys10uv, Thermo). The experiments were repeated three times.

Phase solubility diagrams were obtained by plotting G2 solubility versus CD concentration.

From these curves, a linear regression analysis was done in order to obtain the following equations for G2/HPαCD, G2/MβCD and G2/HPβCD systems, respectively:

$$y = 0.203x + 6 \times 10^{-5} \quad (1)$$

$$y = 0.305x + 5 \times 10^{-5} \quad (2)$$

$$y = 0.326x + 5 \times 10^{-5} \quad (3)$$

where x is the concentration of the corresponding CD and y is the concentration of G2.

2.5. Stoichiometry determination by the continuous variation method (Job's plot)

To determine the stoichiometry of the complexes, the continuous variation technique (Job's method) was adopted (Job, 1928). Aqueous G2 and CDs solutions of equal concentration were mixed in different proportions varying the molar ratio while keeping the total concentration constant (0.2 mM). The differences in absorbance between G2 and the complexes, measured using UV spectrophotometer at 290 nm at 25 °C, were plotted against the

given molar fraction (varying from 0 to 1); the maximum of the curve indicated the stoichiometry.

2.6. ^1H NMR spectroscopy

^1H and ROESY NMR spectra were acquired on a JEOL Eclipse 300 or a Bruker Avance III spectrometer at 300 and 400 MHz, respectively; samples of G2 were referenced relative to the residual methyl peak of CD_3OD at δ 3.31 ppm, while those of the complexes were referenced relative to the residual peak of D_2O at δ 4.80 ppm. ROESY spectra were acquired with a mixing time of 200 ms.

2.7. ESI-mass spectroscopy

Electrospray mass spectrometry experiments were performed with a Bruker Daltonics Esquire 6000 spectrometer with ion trap; data were collected from ca. 5 mM 1:1 G2/CD aqueous solutions.

2.8. X-ray powder diffractometry

Powder X-ray diffractograms of free G2, cyclodextrins, complexes and physical mixtures were obtained from a Siemens Dn 5000 diffractometer using Cu Kα (λ = 1.5406 Å) radiation with 30 mA current and voltage of 35 kV. The instrument operated over the 2θ range of 2–38 °C at a scanning rate of 1 °C/min.

2.9. Differential scanning calorimetry (DSC)

Thermal analyses of free G2, CDs, complexes and physical mixtures were conducted using differential scanning calorimetry. The solid samples were placed in sealed aluminum pans (an empty pan was used as reference) and DSC curves were recorded on a Mettler Toledo DSC 821^e instrument, and then scanned at a heating rate of 5 °C/min over a temperature range of 20–200 °C under 100 mL/min nitrogen constant flow (Veiga, Merino, Fernández, & Lozano, 2002).

2.10. Biological assays

2.10.1. Trypanocidal assay

Two *T. cruzi* strains (NINOA and INC5), isolated from acute and chronic chagasic patients from two different endemic areas of Mexico, were used. Both strains were maintained in the vector *Meccus pallidipennis* (Insecta: Hemiptera), and by serial passages in NIH female mice. Free G2, CDs and the three complexes were evaluated in vitro against bloodstream trypomastigotes of *T. cruzi* according to the method described by Brener (1962).

2.10.2. Antileishmanial activity assay

In vitro tests against promastigotes of *L. mexicana* (MNYC/BZ/62/M379 strain) were performed to evaluate the antileishmanial activity of free G2, CDs and the three complexes. To estimate the 50% inhibition concentration (IC_{50}) the Alamar blue micromethod was used (Mikus & Steverding, 2000).

2.10.3. Cytotoxicity assays

The effect of free G2, CDs and the three complexes on the proliferation of human lymphocytes was evaluated using the Sulphorodamine B method (Skehan et al., 1990).

2.10.4. Hemolysis assays

Freshly drawn blood was obtained from healthy 30–32 years old, non-smoker, and non-medicated male donors. Erythrocytes were separated by centrifugation at 1000 rpm for 5 min, washed 3 times with isotonic phosphate buffer (pH 7.4) and resuspended in the buffer solution to give a hematocrit of 2%. The release of hemoglobin from treated cells with G2, CDs and the three complexes, was measured spectrophotometrically at 543 nm in a microplate reader (Labsystems Multiskan MS). Results were expressed as percentages of hemolysis relative to the absorbance of water treated cells.

Table 1
Solubility of G2 and its CD complexes.

Compound	Solubility (mg/mL)(mean ± SD)	$^aS_{CD}/^bS_{G2}$
G2	0.060 ± 0.001105	–
G2/HPαCD	0.069 ± 0.001252	1.15
G2/MβCD	0.121 ± 0.000847	2.01
G2/HPβCD	0.100 ± 0.000528	1.66

[a] S_{CD}, G2/CD complex solubility.
[b] S_{G2}, G2 solubility.

3. Results and discussion

3.1. Determination of intrinsic solubility

The aqueous solubility of G2 and G2/CDs is presented in Table 1. The greatest change was observed in G2/MβCD, wherein G2 solubility was increased by 50%. With G2/HPβCD, G2 had an increase of 1.6 times. The minimum change was observed with G2/HPαCD system.

3.2. Phase-solubility diagram

Each solubility curve in Fig. 2 can be classified as A_L type (Higuchi & Connors, 1965) since each one of them shows that there is a linear increase in G2 solubility with increasing concentrations of the macrocycle, indicating the association between G2 and CD.

A slope of less than 1 in all profiles (equations shown in Section 2.4) indicates that the solubility increase was due to the formation of a 1:1 complex (Higuchi & Connors, 1965). The apparent stability constant ($K_{1:1}$) was estimated from the straight line of the phase-solubility diagram according to the expression $K_{1:1} = m/So(1-m)$, where m is the slope of the linear plot and So is G2 solubility (So = 0.06 mg/L, 0.000239 M) determined as described in Section 2.3. $K_{1:1}$ is a useful index to compare the affinity of G2 to the different CDs and consequently estimate the binding strength of the complex. The magnitude of $K_{1:1}$ is generally in the range 0–100,000 M^{-1} with 0 being the value for a drug that is incapable of forming an inclusion complex; values less than 100 M^{-1} denote weak guest–host associations, whereas values close to 10,000 M^{-1}

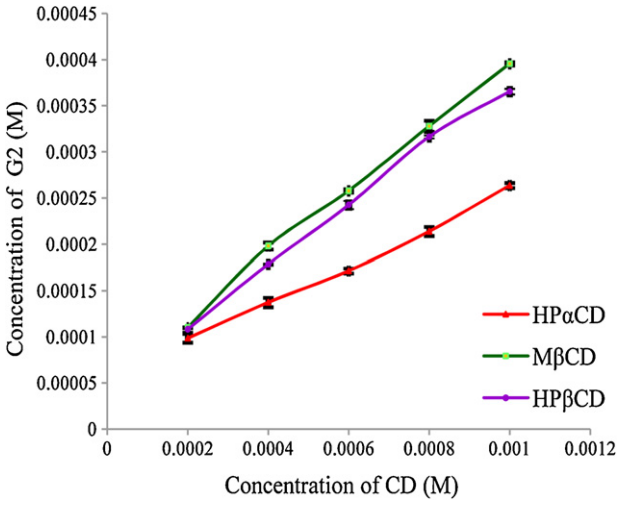

Fig. 2. Phase-solubility diagrams of G2/HPαCD, G2/MβCD and G2/HPβCD systems.

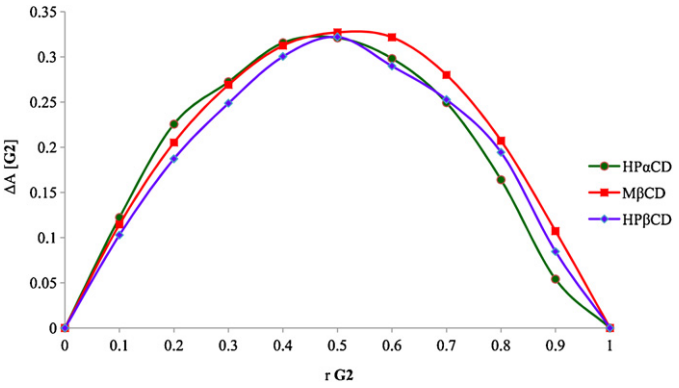

Fig. 3. Continuous variation plot of G2/HPαCD, G2/MβCD and G2/HPβCD systems.

indicate strong interactions, and 100,000 M^{-1} being near the upper value observed experimentally for cyclodextrin complexes of drugs (Rajewski & Stella, 1996). $K_{1:1}$ values for G2/HPαCD, G2/MβCD and G2/HPβCD were 1073, 2266 and 2037 M^{-1}, respectively. This suggests that there was a favorable interplay between G2 and CDs, where G2/MβCD displayed the strongest interaction and thus appears as the most stable system.

Another important aspect of the complexes is the solubilizing efficiency of the CDs in an aqueous vehicle. This can be determined either from the slope of the phase-solubility profile, or from the ratio of the concentration of the dissolved complex to the concentration of the free CD, which is referred to as complexation efficiency (CE) (Loftsson et al., 2005). Thus, CE = slope/1 − slope, where the slope is taken from the phase solubility diagram. The complexation efficiencies for G2/HPαCD, G2/MβCD and G2/HPβCD systems corresponded to 0.255, 0.539 and 0.484, respectively. These values are in agreement with the results obtained in Section 3.1 since G2/MβCD complex showed the highest capacity to increase the guest aqueous solubility.

3.3. Stoichiometry determination by the continuous variation method (Job's plot)

Stoichiometry of the systems was the same for the cyclodextrins used (Fig. 3); the three plots have a maximum value at $r = 0.5$ and a symmetrical shape, indicating that the complexes were formed with 1:1 stoichiometry. These results are in agreement with the outcomes reported on phase-solubility experiments (Section 3.2).

3.4. ^{1}H NMR spectroscopy

The inclusion mode of G2 with the three cyclodextrins was probed by NMR spectroscopy. Due to the poor G2 aqueous solubility, its ^{1}H NMR spectrum was acquired in CD_3OD; the only signal present was a sharp singlet corresponding to the aromatic protons of the benzimidazole nucleus at δ 7.89 ppm, while a broad shoulder near δ 4.90 ppm may be assigned to the NH proton partially exchanged with the deuterated solvent (Supplementary data). Direct comparison of G2 chemical shift relative to the inclusion complex was precluded by the insolubility of benzimidazole in D_2O/CD_3OD (80:20), solvent mixture employed for analysis of the complexes. Nonetheless, the association of one molecule of G2 in the CD cavities was evidenced by the differences in the ^{1}H NMR spectra of the cyclodextrin (Rojas-Aguirre et al., 2011).

In the specific case of G2/HPαCD, the CD signals showed small chemical shift displacements relative to HPαCD. For example, the resonances at δ 4.00 and 3.87 ppm (corresponding to H-3 and H-5, respectively) shift downfield to δ 4.01 and 3.88 ppm, a difference $\Delta\delta$ of 0.01 ppm. Although this appears to indicate that G2 is within the HPαCD cavity, 2D NMR data suggested that the benzimidazole derivative interacts with H-1 located on the oligosaccharide periphery (see below).

Table 2
Chemical shifts of the three CDs and their inclusion complexes with G2.

Assignment	δ (free compound)	δ (complex)	$\Delta\delta$ (complex-free)
HPαCD			
H-1	5.175	5.177	0.002
H-3	3.999	4.006	0.007
H-5	3.867	3.875	0.008
H-2	3.770	3.792	0.022
H-4	3.585	3.597	0.012
Me	1.154	1.157	0.003
Me	1.133	1.141	0.008
MβCD			
H-1	5.148	5.141	−0.007
H-3	3.860	3.860	0.000
H-5	3.773	3.780	0.007
H-2	3.610	3.603	−0.007
H-4	3.595	3.580	−0.015
Me	3.509	3.516	0.007
HPβCD			
H-1	5.132	5.129	−0.003
H-3	3.923	3.930	0.007
H-5	3.797	3.790	−0.007
H-2	3.695	3.697	0.002
H-4	3.536	3.535	−0.001
Me	1.102	1.101	−0.001
Me	1.073	1.080	0.007

The association of G2 with MβCD was also reflected in the displacement of the signal corresponding to H-5 of the cyclodextrin, which have been attributed to the inclusion of guest. Likewise, the signal corresponding to H-3 of HPβCD shifts to lower field in G2/HPβCD, likely due to inclusion of G2 through the wide side of the cyclodextrin (Table 2). The spectra of the three complexes are shown in Supplementary data.

Detailed information on the mode of interaction of G2 with CDs was obtained by 2D NMR experiments. Rotating-frame NOE spectroscopy (ROESY) provided information on the spatial proximity of G2 with CDs. ROESY spectra of G2/HPαCD, G2/MβCD and G2/HPβCD systems were acquired in 80:20 D_2O/CD_3OD mixtures. The contour plots revealed that the singlet corresponding to G2 aromatic protons had intermolecular cross-peaks with CDs protons, in all cases. For G2/HPαCD, the peak had a weak intermolecular interaction with H-1 of HPαCD at δ 5.177 ppm (Supplementary data). This indicates that G2 might form a non-inclusion complex through hydrogen bonding on the outer surface of the oligosaccharide (Brewster & Loftsson, 2007). Although this observation is valid for the solvent system employed in NMR measurements, further support for the weak interaction between G2 and HPαCD in aqueous solution is given by the small $K_{1:1}$ value determined by phase-solubility.

In the case of G2/MβCD, the strongest interactions were given between G2 aromatic protons and H-3 and H-5 of the CD, which overlap in a broad signal in the ^{1}H NMR spectrum (Supplementary data). Thus, G2 appears to be completely included within the cavity, with G2 aromatic protons in the proximity of H-3 and H-5. These observations agree with the favorable association determined by phase-solubility studies.

The ROESY spectrum of G2/HPβCD is characterized by an intermolecular interaction of G2 aromatic protons with H-5 on the narrow rim of the macrocycle. Interestingly, G2 had another cross-peak that appears to be correlated with H-7 of the hydroxypropyl pendant arms (Fig. 4). Moreover, the strongest cross-peaks in the spectrum corresponded to interactions between CH_3 of the hydroxypropyl arms, centered at δ 1.091, with H-3 and H-5 of HPβCD (Fig. 4c), placing the hydroxypropyl groups entirely within the cavity. Inclusion of the hydroxypropyl substituents within the CD has

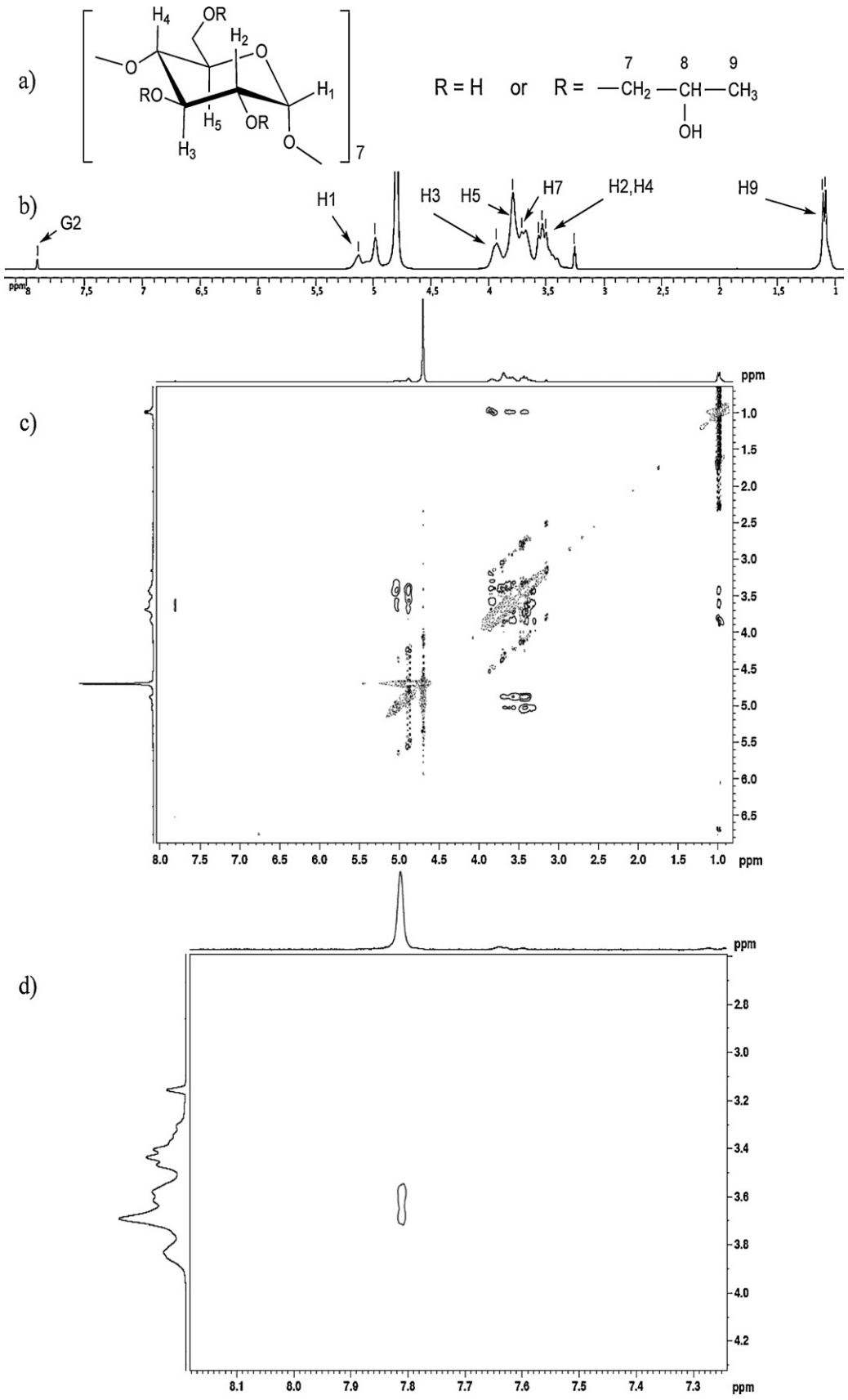

Fig. 4. (a) Identification of HPβCD protons; (b) ^{1}H NMR spectrum of G2/HPβCD; (c) ROESY spectrum of G2/HPβCD; (d) section of the ROESY spectrum with cross peaks between the benzimidazole and H-5 of HPβCD.

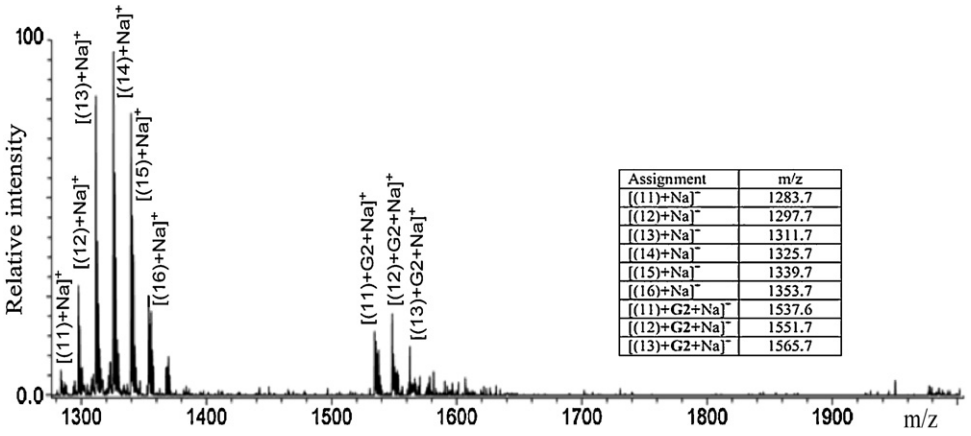

Assignment	m/z
[(11)+Na]+	1283.7
[(12)+Na]+	1297.7
[(13)+Na]+	1311.7
[(14)+Na]+	1325.7
[(15)+Na]+	1339.7
[(16)+Na]+	1353.7
[(11)+G2+Na]+	1537.6
[(12)+G2+Na]+	1551.7
[(13)+G2+Na]+	1565.7

Fig. 5. Electrospray mass spectrum of G2/MβCD in aqueous solution; numbers shown in brackets refer to the number of methyl groups bound to the CD.

been previously observed (Harata, Rao, Pitha, Fukunaga, & Uekama, 1991), suggesting that this substituent may compete for inclusion with potential guest molecules. A reasonable interpretation of the ROESY spectrum in Fig. 4 would place the hydroxypropyl arms inside the cavity, and therefore strongly interacting with H-3 and H-5, whereas G2 would be partially included through the cyclodextrin narrow side, placing it in the proximity of both H-5 of the oligosaccharide structure and H-7 of the hydroxypropyl groups.

3.5. ESI-mass spectroscopy

ESI-mass spectrometry was also used to assess qualitatively the G2 and CDs species present in solutions at 1:1 molar ratio. The experiments provided information on the extent of non-covalent interactions, as well as on the stoichiometry of the inclusion complexes, when they were present (De Paula et al., 2011; Rekharsky, Inoue, Tobey, Metzger, & Anslyn, 2002; Toma et al., 2004). In the case of G2/HPαCD, the spectrum did not differ from that of HPαCD, indicating that no inclusion complex was formed. Thus, the observed distribution of peaks between m/z = 1111.5–1517.8 corresponded to sodium cationized HPαCD with 2–9 hydroxypropyl groups (Supplementary data). In contrast, G2/MβCD spectrum was clearly distinct of MβCD. Macrocyclic solutions gave rise to six major peaks between m/z = 1283.7–1353.7, which correspond to sodium cationized MβCD. G2/MβCD spectrum showed additional peaks at m/z = 1537.6, 1551.7, and 1565.7, which were assigned to inclusion complex of CD with 11, 12, and 13 methyl groups: $[(11)+G2+Na]^+$, $[(12)+G2+Na]^+$, and $[(13)+G2+Na]^+$. These experimental data revealed the dominant inclusion complexes with 1:1 stoichiometry; moreover, it appears that MβCD with a lower methylation degree were more capable of hosting the benzimidazole derivative (Fig. 5).

With respect to the HPβCD spectrum, nine peaks were observed between m/z = 1215.5–1679.8, which correspond to sodium cationized CDs with 1–9 hydroxypropyl groups. The G2/HPβCD spectrum displayed additional peaks at m/z = 1527.5, 1585.6 and 1643.7, associated with the inclusion complexes: $[(2)+G2+Na]^+$, $[(3)+G2+Na]^+$ and $[(4)+G2+Na]^+$ (Supplementary data). As in the case of MβCD, a low degree of substitution with 2–4 hydroxypropyl groups creates an environment that is not sterically demanding that hinders the association with G2.

3.6. X-ray diffraction analysis

Powder X-ray diffraction allows the identification of a complexation process due to the differences between the diffraction patterns of solid state complex and those of the components (Muñoz-Botella et al., 1996; Veiga, Teixeira-Dias, Kedzierewicz, Sousa, & Mincent, 1996). Visual inspection of Fig. 6Ia indicates that G2 has a diffraction pattern which consists of several high intensity peaks, demonstrating the crystalline character of the compound, in contrast to amorphous character of HPαCD (Fig. 6Ib), MβCD and HPβCD (Supplementary data). The XRD pattern of PM prepared from HPαCD and G2 (Fig. 6Ic) clearly shows the peaks corresponding to the superposition of the diffractograms of the individual components; this behavior is also observed with the other mixtures (Supplementary data). On the other hand, none of the inclusion complexes displayed the characteristic peaks of G2 and the observed amorphous halo is indicative of the association process (Fig. 6Id and Supplementary data) (Muñoz-Botella et al., 1996).

3.7. Differential scanning calorimetry

Differential scanning calorimetry (DSC) was used to confirm complex formation. Visual inspection of Fig. 6IIa reveals a sharp endothermic peak, typical of a crystalline material at 238 °C, corresponding to G2 melting point; a second endotherm shows decomposition (260 °C) (Hernández-Luis et al., 2010). The endothermic peaks at 53–54 °C in the DSC diagrams of CDs are attributed to the loss of a varying number of water molecules (Fig. 6IIb for HPαCD; for MβCD and HPβCD see Supplementary data), which can be surrounding the CD or inside the cavity (Fini, Ospitali, Zoppetti, & Puppini, 2008; Veiga et al., 2002); no decomposition of the CDs is observed. The curve of PM of G2 and HPαCD (Fig. 6IIc) shows a shift of the melting point and decomposition endotherm of G2 to 190 °C and 284 °C, respectively. A similar change in the thermal profile of G2 was observed in the PM of G2 and HPβCD, since the G2 sharp peak was shifted to 187 °C. With respect to PM of G2 and MβCD, a less notorious change was observed since a small peak is present at 227 °C (Supplementary data). Thermograms of inclusion complexes showed a change related to the large and broad peaks corresponding to the loss of water suggesting that dehydration of the complexes occurs over a large temperature range. Those water molecules are likely hydrogen-bonded to the CD OH groups outside the cavity (Fini et al., 2008), with different degrees of binding strength, and therefore are freed in a large range of temperatures. On the other hand, the absence of the melting point peak in the G2/MβCD and G2/HPβCD systems, is indicative that the formation of new amorphous entities has occurred. With respect to G2/HPαCD a different situation is observed (Fig. 6IId); the endotherm corresponding to G2 melting point is still present. Although the peak is not as intense as for free G2, it suggests that an inclusion complex may not be formed.

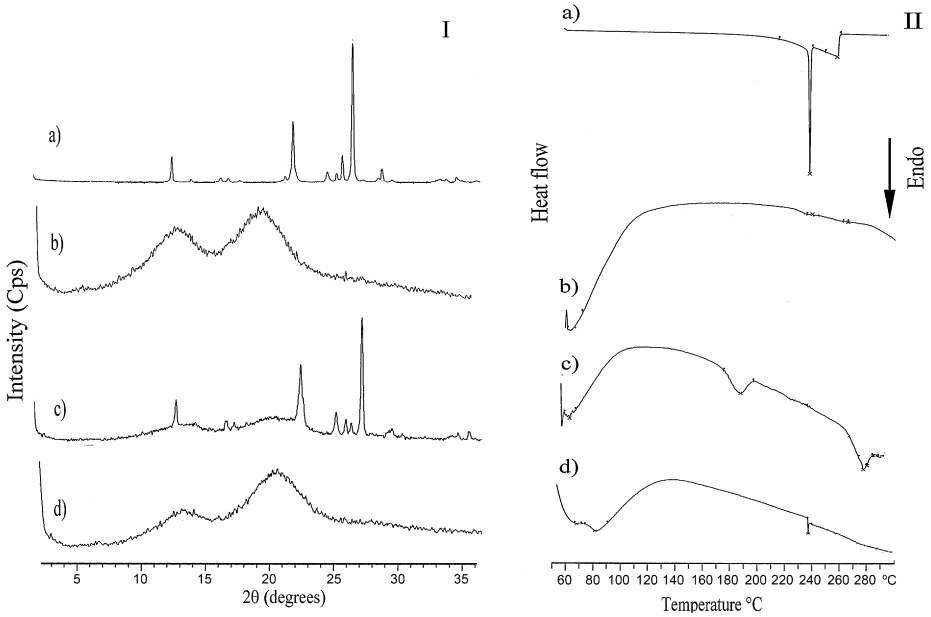

Fig. 6. (I) Powder X-ray diffractograms: (a) G2; (b) HPαCD; (c) G2/HPαCD PM; (d) G2/HPαCD complex. (II) DSC thermograms: (a) G2; (b) HPαCD; (c) G2/HPαCD PM; (d) G2/HPαCD complex.

Despite DSC experiments being part of the solid-state characterization, this result is in agreement with the observations made by NMR spectroscopy.

3.8. Antiparasitic activity

The in vitro leishmanicidal activities of G2, G2/HPαCD, G2/MβCD and G2/HPβCD, against promastigotes of *L. mexicana* are shown in Table 3, with Amphotericin B and Glucantime as references. Although G2 displayed antileishmanial activity, its performance was not better than the drug references. However, the three G2/CD systems showed a surprising augment in antileishmanial activity. G2/HPαCD and G2/HPβCD had a comparable behavior with IC_{50} of 5.1 and 4.9 μg/mL, respectively. In contrast, G2/MβCD displayed an IC_{50} of 1.9 μg/mL, enormously surpassing not only the increased activity of the other systems, but also the activity of Amphotericine B and Glucantime. It is important to note that HPαCD, MβCD and HPβCD had activity that could contribute to the antiparasitic effect of the G2/CD associations. The most active was HPβCD, although G2/HPβCD was not as high as G2/MβCD.

Table 3 also presents the results of the trypanocidal activity assays of G2, G2/HPαCD, G2/MβCD and G2/HPβCD. In this case, free G2 had a higher activity than Nifurtimox and Benznidazole (drug references) despite its poor solubility in the vehicle (water/ethanol 99:01). Regrettably, the activity of G2/HPαCD decreased in comparison to free G2, while the activity of G2/HPβCD was comparable to drug references. Nonetheless, G2/MβCD demonstrated to be the best system to enhance the trypanocidal activity because it exceeded the activity of reference drugs, as happened in the antileishmanial trials. Contrary to the activities observed for the CDs in antileshmanial assays, HPβCD had the smallest contribution, followed by HPαCD, and finally by MβCD. Moreover, the activity of the latter increased as a function of the concentration; consequently, it seems that there is an additive effect between MβCD and G2 trypanocidal activity.

Further studies must be done to determine the reason for the activity of the CDs, although it can be tentatively argued that these oligosaccharides disrupt the membrane of the parasites (Kiss et al., 2010).

In both assays, the least active system was G2/HPαCD. This result is in agreement with all the physicochemical analyses reported above. Although this system could be functioning as drug carrier when tested against *L. mexicana*, it did not work as such against *T. cruzi*. In the case of G2/MβCD, it is noteworthy that this complex had the highest $K_{1:1}$ and solubility, therefore acted as the best drug carrier. This can be explained based on reports that MβCD reduces the barrier function and thereby enhance drug delivery through biological membranes (Loftsson, Vogensen, & Brewster, 2007), resulting in the highest antiprotozoal activity observed in this work.

Table 3
Antiparasitic activity of G2 and the complexes against *T. cruzi* and *L. mexicana*.

Compound	% lysis *T. cruzi* Concentration (μg/mL)				IC_{50} (μM) *L. mexicana*
	5	10	50	100	
HPαCD	36.9	30.9	41.7	30.6	16
MβCD	6.1	18	23.4	39.6	18.5
HPβCD	9.4	11	15.3	10.8	5.8
G2/HPαCD	8.3	77	29.9	13.7	5.1
G2/MβCD	12.6	39	57.4	82.7	1.9
G2/HPβCD	26.1	7.8	9.9	41.7	4.9
G2	5.6	16.9	51.4	58.4	31.3
Nifurtimox	0	33	45	50	–
Benznidazole	0	4.5	16	43	–
Amphotericin B	–	–	–	–	6.5
Glucantime	–	–	–	–	18.4

3.9. Cytotoxicity and hemolytic assays

Although numerous works have determined the toxicity of CDs (Gould & Scott, 2005; Kiss et al., 2010; Loftsson & Duchêne, 2007; Salem et al., 2009), the study of inclusion complexes on human lymphocytes and erythrocytes has been the most relevant, mainly because an augment of compound aqueous solubility could generate a change in its toxicity profile. Fig. 7I reveals that neither G2 nor G2/CDs systems affected cell proliferation of human lymphocytes at any concentration tested. The hemolytic activity was evaluated at 10–500 μM and not more than 25% of hemolysis was detected.

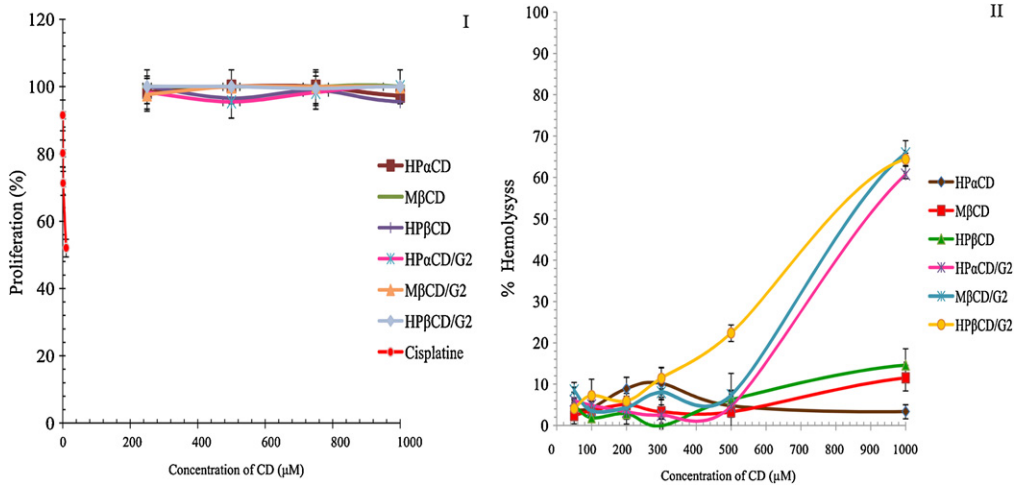

Fig. 7. Cytotoxicity assays. (I) Effect of G2/CD systems on lymphocyte cell proliferation. (II) G2/CD hemolytic activity on human erythrocytes.

Nonetheless, from 500–1000 μM, the hemolytic activity increased linearly with G2/CD concentrations; this effect can be attributed to G2 since CDs did not show hemolytic activity at this concentration range (Fig. 7II). These results were favorable since the maximum G2/CD concentration for antiprotozoal activity tests was 390 μM (100 μg/mL), concentration where G2/CD systems were completely safe.

4. Conclusion

We have confirmed the formation of supramolecular association structures between G2 and the three modified CDs. ^{1}H NMR data and ESI-mass spectrometry indicated that three different modes of interaction between G2 and modified CDs were possible. The first type consisted of a non-inclusion complex between G2 and HPαCD; the second type consisted of a conventional inclusion complex between G2 and MβCD, akin to the most commonly reported works. The third type of interaction was a partial inclusion through the narrow side of G2 and HPβCD. All the data obtained from the NMR spectroscopy, ESI-mass spectrometry and solubility studies, as well as solid state characterization, correlated with the observed results in the antiparasitic trials since the enhancement in biological activity was G2/MβCD > G2/HPβCD > G2/HPαCD. It is noteworthy that G2/CDs showed no cytotoxicity at the concentrations tested as antiparasitic agents. Finally, results indicate that G2/MβCD is a good alternative of G2 formulation to further biological evaluations.

Acknowledgments

We are grateful to Margarita Portilla, Elvia Reynoso and Cecilia Salcedo from Facultad de Química, USAI, UNAM, for the determination of DSC thermograms and powder X-ray diffractograms, and Beatriz Quiroz-García from IQ, UNAM, for assistance with NMR spectroscopy. This study was supported by grants from PAPIIT-UNAM IN210809 and CONACyT 80093.

Appendix A. Supplementary data

Supplementary data associated with this article can be found, in the online version, at doi:10.1016/j.carbpol.2011.08.009.

References

Anonymous (2011). http://www.who.int/neglected_diseases/diseases/en/ Accessed May 2011.
Baka, E., Comer, J., & Takács-Novák, K. (2008). Study of equilibrium solubility measurement by saturation shake-flask method using hydrochlorothiazide as model compound. *Journal of Pharmaceutical and Biomedical Analysis*, *46*(2), 335–341.
Brener, Z. (1962). Therapeutic activity and criterion of cure on mice experimentally infected with *Trypanosoma cruzi*. *Revista do Instituto de Medicina Tropical de São Paulo*, *4*, 389–396.
Brewster, M. E., & Loftsson, T. (2007). Cyclodextrins as pharmaceutical solubilizers. *Advanced Drug Delivery Reviews*, *59*(7), 645–666.
Carrier, R. L., Miller, L. A., & Ahmed, I. (2007). The utility of cyclodextrins for enhancing oral bioavailability. *Journal of Controlled Release*, *123*(2), 78–99.
Clayton, J. (2010). Chagas disease 101. *Nature*, *465*(7301), S4–S5.
Coura, J., & Pinto, J. C. (2009). Epidemiology, control and surveillance of Chagas' disease: 100 years after its discovery. *Memórias do Instituto Oswaldo Cruz*, *104*(Suppl. I), 31–40.
Croft, S. L., Barrett, M. P., & Urbina, J. A. (2005). Chemotherapy of trypanosomiasis and leishmaniasis. *Trends in Parasitology*, *21*(11), 508–512.
Croft, S. L., & Coombs, G. H. (2003). Leishmaniasis: Current chemotherapy and recent advances in the search for novel drugs. *Trends in Parasitology*, *19*(11), 502–508.
Csempesz, F., Süle, A., & Puskás, I. (2010). Induced surface activity of supramolecular cyclodextrin–statin complexes: Relevance in drug delivery. *Colloids and Surfaces A: Physicochemical and Engineering Aspects*, *354*(1–3), 308–313.
Danel, C., Azaroual, N., Brunel, A., Lannoy, D., Vermeersch, G., Odou, P., et al. (2008). Study of the complexation of risperidone and 9-hydroxyrisperidone with cyclodextrin hosts using affinity capillary electrophoresis and ^{1}H NMR spectroscopy. *Journal of Chromatography A*, *1215*(1–2), 185–193.
De Paula, W., Denadai, Â., Santoro, M., Braga, A., Santos, R., & Sinisterra, R. (2011). Supramolecular interactions between losartan and hydroxypropyl-β-CD: ESI mass-spectrometry. NMR techniques, phase solubility, isothermal titration calorimetry and anti-hypertensive studies. *International Journal of Pharmaceutics*, *404*(1–2), 116–123.
Desjeux, P. (2004). Leishmaniasis: Current situation and new perspectives. *Comparative Immunology, Microbiology and Infectious Diseases*, *27*(5), 305–318.
Dodziuk, H. (2006). Molecules with holes – cyclodextrins. In H. Dodziuk (Ed.), *Cyclodextrins and their complexes* (pp. 1–20). Germany: Wiley-VCH.
Fini, A., Ospitali, F., Zoppetti, G., & Puppini, N. (2008). ATR/Raman and fractal characterization of HPBCD/progesterone complex solid particles. *Pharmaceutical Research*, *25*(9), 2030–2040.
Gould, S., & Scott, R. (2005). 2-Hydroxypropyl-β-cyclodextrin (HP-β-CD): A toxicology review. *Food and Chemical Toxicology*, *43*(10), 1451–1459.
Gyapong, J. O., Gyapong, M., Yellu, N., Anakwah, K., Amofah, G., Bockarie, M., et al. (2010). Integration of control of neglected tropical diseases into health-care systems: Challenges and opportunities. *Lancet*, *375*, 160–165.
Harata, K., Rao, C. T., Pitha, J., Fukunaga, K., & Uekama, K. (1991). Crystal structure of 2-*O*-[(S)-2-hydroxypropyl]cyclomaltoheptaose. *Carbohydrate Research*, *222*(1), 37–45.
Hernández-Luis, F., Hernández-Campos, A., Castillo, R., Navarrete-Vázquez, G., Soria-Arteche, O., Hernández-Hernández, M., et al. (2010). Synthesis and biological activity of 2-(trifluoromethyl)-1*H*-benzimidazole derivatives against some protozoa and *Trichinella spiralis*. *European Journal Medicinal Chemistry*, *45*(7), 3135–3141.
Higuchi, T., & Connors, K. A. (1965). Phase solubility techniques. *Advances in Analytical Chemistry and Instrumentation*, *4*, 117–212.
Iatropoulos, M. J., Wang, C. X., von Keutz, E., & Williams, G. M. (2006). Assessment of chronic toxicity and carcinogenicity in an accelerated cancer bioassay in

rats of Nifurtimox, an antitrypanosomiasis drug. *Experimental and Toxicologic Pathology*, *57*(5–6), 397–404.

Job, P. (1928). Formation and stability of inorganic complexes in solution. *Annali di Chimica Applicata*, *9*, 113–203.

Kiss, T., Fenyvesi, F., Bácskay, I., Iványi, R., Váradi, J., Fenyvesi, E., et al. (2010). Evaluation of the cytotoxicity of β-cyclodextrin derivatives: Evidence for the role of cholesterol extraction. *European Journal of Pharmaceutical Science*, *40*(4), 376–380.

Lannes-Vieira, J., Correia, M., Corrêa-Oliveira, R., & de Araújo-Jorge, T. C. (2009). Chagas disease centennial anniversary celebration: Historical overview and prospective proposals aiming to maintain vector control and improve patient prognosis – a permanent challenge. *Memórias do Instituto Oswaldo Cruz*, *104*(Suppl. I), 5–7.

Loftsson, T., & Duchêne, D. (2007). Cyclodextrins and their pharmaceutical applications. *International Journal of Pharmaceutics*, *329*(1–2), 1–11.

Loftsson, T., Hreinsdóttir, D., & Másson, M. (2005). Evaluation of cyclodextrin solubilization of drugs. *International Journal of Pharmaceutics*, *302*(12), 18–28.

Loftsson, T., Vogensen, S., & Brewster, M. (2007). Effects of cyclodextrins on drug delivery through biological membranes. *Journal of Pharmaceutical Science*, *96*(10), 2532–2546.

Maya, J. D., Bollo, S., Nuñez-Vergara, L. J., Squella, J. A., Repetto, Y., Morello, et al. (2003). *Trypanosoma cruzi*: Effect and mode of action of nitroimidazole and nitrofuran derivatives. *Biochemical Pharmacology*, *65*, 999–1006.

Mikus, J., & Steverding, D. (2000). A simple colorimetric method to screen drug cytotoxicity against Leishmania using the dye Alamar Blue. *Parasitology International*, *48*(3), 265–269.

Muñoz-Botella, S., del Castillo, B., Martìn, M. A., Menéndez, J. C., Vázquez, L., & Lerner, D. A. (1996). Analytical applications of retinoid-cyclodextrin inclusion complexes. 1. Characterization of a retinal-β-cyclodextrin complex. *Journal of Pharmaceutical and Biomedical Analysis*, *14*(8–10), 909–915.

Natera, S., Machuca, C., Padrón-Nieves, M., Romero, A., Díaz, E., & Ponte-Sucre, A. (2007). *Leishmania* spp.: Proficiency of drug-resistant parasites. *International Journal of Antimicrobial Agents*, *29*(6), 637–642.

Navarrete-Vázquez, G., Cedillo, R., Hernández, A., Yépez, L., Hernández-Luis, F., Valdéz, J., et al. (2001). Synthesis and antiparasitic activity of 2-(trifluoromethyl)-benzimidazole derivatives. *Bioorganic and Medicinal Chemistry Letters*, *11*(2), 187–190.

Navarrete-Vázquez, G., Rojano-Vilchis, M., Yépez-Mulia, L., Meléndez, V., Gerena, L., Hernández-Campos, A., et al. (2006). Synthesis and antiprotozoal activity of some 2-(trifluoromethyl)-1*H*-benzimidazole bioisosteres. *European Journal of Medicinal Chemistry*, *41*(1), 135–141.

Navarrete-Vázquez, G., Yépez-Mulia, L., Hernández-Campos, A., Tapia, A., Hernández-Luis, F., Cedillo, R., et al. (2003). Synthesis and antiparasitic activity of albendazole and mebendazole analogues. *Bioorganic and Medicinal Chemistry*, *11*(21), 4615–4622.

Rajewski, R. A., & Stella, V. J. (1996). Pharmaceutical applications of cyclodextrins. 2. In vivo drug delivery. *Journal of Pharmaceutical Science*, *85*(11), 1142–1169.

Rekharsky, M., Inoue, Y., Tobey, S., Metzger, A., & Anslyn, E. (2002). Ion-pairing molecular recognition in water: Aggregation at low concentrations that is entropy-driven. *Journal of the American Chemical Society*, *124*(50), 14959–14967.

Renslo, A. R., & McKerrow, J. H. (2006). Drug discovery and development for neglected parasitic diseases. *Nature Chemical Biology*, *2*(12), 701–710.

Rojas-Aguirre, Y., Yépez-Mulia, L., Castillo, I., López-Vallejo, F., Soria-Arteche, O., Hernández-Campos, A., et al. (2011). Studies on 6-chloro-5-(1-naphthyloxy)-2-(trifluoromethyl)-1H-benzimidazole/2-hydroxypropyl-β-cyclodextrin association: Characterization, molecular modeling studies, and in vivo anthelminthic activity. *Bioorganic and Medicinal Chemistry*, *19*(2), 789–797.

Salem, B. L., Bosquillon, C., Dailey, L. A., Delattre, L., Martin, G. P., Evrard, B., et al. (2009). Sparing methylation of β-cyclodextrin mitigates cytotoxicity and permeability induction in respiratory epithelial cell layers in vitro. *Journal of Controlled Release*, *136*(2), 110–116.

Santos, D., Coutinho, C., Madeira, M. F., Bottino, C. G., Vieira, R. T., Nascimento, S. B., et al. (2008). Leishmaniasis treatment, a challenge that remains: A review. *Parasitology Research*, *103*(1), 1–10.

Skehan, P., Storeng, R., Scudiero, D., Monks, A., McMahon, J., Vistica, D., et al. (1990). New colorimetric cytotoxicity assay for anticancer-drug screening. *Journal of the National Cancer Institute*, *82*(13), 1107–1112.

Toma, S. H., Uemi, M., Nikolaou, S., Tomazela, D. M., Eberlin, M. N., & Toma, H. E. (2004). {Trans-1,4-bis[(4-pyridyl)ethenyl]benzene}(2,2-bipyridine)ruthenium(II) complexes and their supramolecular assemblies with beta-cyclodextrin. *Inorganic Chemistry*, *43*(11), 3521–3527.

Tong, W., & Wen, H. (2008). Applications of complexation in the formulation of insoluble compounds. In R. Liu (Ed.), *Water-insoluble drug formulation* (2nd ed., pp. 146–154). Boca Raton, FL: CRC Press.

Veiga, F., Teixeira-Dias, J. C., Kedzierewicz, F., Sousa, A., & Mincent, P. (1996). Inclusion complexation of tolbutamide with β-cyclodextrin and hydroypropyl-β-cyclodextrin. *International Journal of Pharmaceutics*, *129*(1–2), 63–71.

Veiga, M. D., Merino, M., Fernández, D., & Lozano, R. (2002). Characterization of some cyclodextrin derivatives by thermal analysis. *Journal of Thermal Analysis*, *68*, 511–516.